Reversible Dissociation and Unfolding of the *Escherichia coli* Aspartate Receptor Cytoplasmic Fragment†

Jiongru Wu,‡ David G. Long,§,|| and Robert M. Weis*,‡,§

Department of Chemistry and Graduate Program in Molecular and Cellular Biology, University of Massachusetts, Amherst, Massachusetts 01003

Received October 10, 1994; Revised Manuscript Received December 21, 1994⊗

ABSTRACT: The thermal denaturation of a 31-kDa soluble fragment derived from the *Escherichia coli* aspartate receptor cytoplasmic region (c-fragment) was found to be reversible. Denaturation monitored by differential scanning calorimetry (DSC) and circular dichroism (CD) was typically over 90% reversible in pH 7.0 buffer. The wild-type c-fragment exhibited one transition (T_m = 51 °C), which was taken as the main denaturation transition. c-Fragments derived from signaling mutants, shown to form oligomers by gel filtration chromatography (GFC), displayed a second low-temperature transition that correlated with the disappearance of the oligomeric form in the GFC traces over the same temperature range. The CD and DSC experiments also indicated that oligomers were more folded than monomers, observations that may provide an explanation for the structural basis of the smooth-swimming signaling state of the receptor. Octyl glucoside (OG), phospholipid (PL), and glycerol were added to characterize factors that contribute to c-fragment stability. At 10 mg/mL OG, the van't Hoff enthalpy of unfolding was reduced ca. 10-fold, although at room temperature the CD spectrum indicated little change in the secondary structure. The van't Hoff enthalpy was not affected by 35% (w/v) glycerol, but the T_m increased by ca. 18 °C. Cooperative transitions were detected in buffer containing OG, PL, and glycerol (10 mg/mL, 2 mg/mL, 35%, respectively). The correlation between conditions where cooperative transitions are observed, and where aspartate-modulated receptor signaling has been previously observed, provides an explanation for the inhibition of signaling in OG-containing buffers without glycerol and PL.

The transmembrane receptor proteins from the chemosensory system of *Escherichia coli* and *Salmonella typhimurium* have proven to be useful in studies of transmembrane signaling since they are comparatively small and simple (for reviews of the chemotaxis system see Bourret et al., 1991; Stock et al., 1991; Parkinson, 1993). Four homologous receptors have been identified in *E. coli* which are homodimers composed of a single 60-kDa polypeptide chain and which enable bacteria to respond to environmental stimuli. The aspartate receptor, Tar,[1] mediates an attractant response to aspartate, and the *E. coli* Tar protein also mediates attractant responses to phenol (Tso & Adler, 1974) and maltose through the maltose binding protein (Dahl & Manson, 1985). Tar and its homologues have been the subject of numerous studies using mutagenesis and biochemical techniques that have established its membrane topology and functional organization. (For a review of the chemotaxis receptors, see Hazelbauer, 1992.)

The aspartate receptor is divided into three functional domains: a periplasmic domain responsible for specific ligand binding, a transmembrane domain defined by two membrane-spanning helices per polypeptide chain, and a highly-conserved cytoplasmic signaling domain which regulates the activity of the cellular signaling cascade. In the crystal structure of the periplasmic ligand-binding domain from the aspartate receptor of *S. typhimurium*, the aspartate binding pocket was found at the interface between two subunits arranged as a dimer (Milburn et al., 1991; Yeh et al., 1993). Site-specific disulfide bond formation has been used to extend the structure of the ligand-binding domain into the membrane, and a model for the arrangement of the four transmembrane helices in the dimer has been constructed (Pakula & Simon, 1992). These structural studies provide further evidence for the dimeric nature of the receptor (Milligan & Koshland, 1988) and its role as the functional unit in transmembrane signaling.

In contrast to the ligand-binding domain and the transmembrane region, less is known of the structure of the cytoplasmic domain of the receptor. Most of the information regarding the c-fragment comes from studies of two functional regions in the cytoplasmic domain: the sites of methylation and the highly-conserved signaling region. Adaptation to stimuli is achieved by reversible methylation of the γ-carboxyl group on certain glutamate residues in the cytoplasmic domain (Terwilliger et al., 1983; Kehry et al., 1983; Nowlin et al., 1987). The transfer of methyl groups from *S*-adenosylmethionine to the receptor is catalyzed by a methyltransferase (CheR), and the hydrolysis of the γ-glutamyl methyl esters to methanol and glutamate is catalyzed by a methylesterase (CheB). From an analysis of the methylation consensus sequence, the secondary structure in this region was postulated to be α-helical (Terwilliger et al., 1986;

† This research was supported by NIH Grant GM-42636, NIH Biomedical Research Support Grant RR-07048, and a Beckman Young Investigator Award (R.M.W.).

* To whom correspondence and reprint requests should be addressed at the Department of Chemistry.

|| Deceased.

‡ Department of Chemistry.

§ Graduate Program in Molecular and Cellular Biology.

⊗ Abstract published in *Advance ACS Abstracts,* February 15, 1995.

[1] Abbreviations: Tar, aspartate receptor; DSC, differential scanning calorimetry; CD, circular dichroism; GFC, gel filtration chromatography, CMC, critical micelle concentration; OG, octyl β-D-glucopyranoside.

0006-2960/95/0434-3056$09.00/0

Table 1: Properties of c-Fragments[a]

mutation (phenotype)[b]	cluster formation[c]	T_m^{dissoc} (°C)	ΔH_{cal}^{dissoc} (kcal/mol)	T_m^{den} (°C)	ΔH_{cal}^{den} (kcal/mol)	ΔH_{vH}^{den} (kcal/mol)	$\Delta H_{vH}^{den}/\Delta H_{cal}^{den}$
wild-type (r)	no			50.6 ± 0.5 (3)	54 ± 7 (4)	36 ± 2 (4)	0.7 ± 0.2[e]
E301K (s)	no			51.5	45.9	32.9	0.7
T311I (s)	yes	34.5	15.4	50.8	54	36	0.7
S325L (s)	yes	38.3	23.2	50.0	38.2	42.8	1.1
V346M (t)	no			50.3	42.3	33.5	0.8
V433I (t)	no			51.2	50.3	35.9	0.7
A436V (t)	no	*(31 ± 2 (6)*	*10 ± 10 (6))*[d]	53.7 ± 0.7 (6)	38 ± 9 (6)	44 ± 3 (6)	1.2 ± 0.3
S461L (s)	yes	46 ± 5 (6)	12.4 ± 0.4 (6)	59.9 ± 0.5 (7)	61 ± 11 (7)	61 ± 4 (7)	1.0 ± 0.3

[a] Where data were averaged, errors are expressed as standard deviations and the number of samples is given in parentheses. For data parameters derived from a single experiment (e.g., E301K), the errors are comparable. [b] Mutations and swimming phenotypes were determined by Mutoh et al. (1986). Key: s, smooth-swimming; t, tumbling; r, random (alternation between smooth-swimming and tumbling). [c] Cluster formation was detected by gel filtration chromatography in pH 7.0 buffer (Long & Weis, 1992). [d] Although previous studies using GFC (Long & Weis, 1992) indicated no evidence for reversible oligomer formation, a low-temperature transition was observed by DSC. [e] The relative uncertainty was estimated from the sum of the ratios of the standard deviation to the mean: $SD(\Delta H_{vH}^{den})/\Delta \bar{H}_{vH}^{den} + SD(\Delta H_{cal}^{den})/\bar{H}_{cal}^{den}$.

Nowlin et al., 1988), and using a structure prediction algorithm based on primary sequence, these portions of the cytoplasmic region are predicted to adopt a coiled-coil structure (Lupas et al., 1991).

The importance of the cytoplasmic region in coupling the receptor to the intracellular signaling cascade was affirmed by mutagenesis studies of the aspartate and the serine receptors, which resulted in chemotaxis null mutations that localized to the cytoplasmic region of the receptor (Mutoh et al., 1986; Ames & Parkinson, 1988). Many of these null mutants "locked" the receptor into either the smooth-swimming or the tumble signaling state; i.e., certain single amino acid substitutions in the cytoplasmic region were sufficient to alter the receptor so that it mimicked either the smooth signaling state (which is normally produced by attractant binding) or the tumble signaling state (which is produced when the attractant concentration decreases abruptly). Most of these mutations occurred within the highly-conserved cytoplasmic region found in the serine and aspartate receptors, the region which interacts with the CheW and CheA proteins of the response cascade (Liu & Parkinson, 1991; also reviewed in Bourret et al., 1991). When the cytoplasmic region of the receptor was expressed as a 31-kDa soluble protein, and the effects of the bias mutations were studied *in vivo*, the mutations produced some of the same effects on signaling as they did in the intact receptor, providing evidence that this soluble protein retained the signaling activity found in the intact receptor (Oosawa et al., 1988). Previously we reported that the smooth mutant forms of the c-fragment had a stronger tendency to cluster in solution than either the wild-type or tumble forms (Long & Weis, 1992). Here we report that the smooth-swimming mutant forms of the c-fragment possess an additional low-temperature transition detectable by DSC and CD spectroscopy which is correlated with the disappearance of the oligomeric form of the c-fragment. These results provide additional evidence of stronger subunit interactions in the cytoplasmic region of the receptor in its attractant-bound form, and that modulating the strength of subunit interactions may play an essential role in the mechanism of transmembrane signaling by the aspartate receptor.

The reconstitution of receptor activity *in vitro* greatly facilitates the thorough analysis of transmembrane signaling. Membranous receptor samples are inherently problematic in transbilayer coupling studies where two different ligand molecules bind to the receptor on opposite sides of the membrane, since both ligand binding sites are unlikely to be simultaneously accessible. Although detergent-solubilized receptor may solve this problem in principle, in practice this has proven difficult to achieve. The Tar receptor solubilized in detergent was found to be inactive, but transmembrane signaling activity, quantified by an attractant-stimulated increase in the rate of receptor methylation, could be restored in a mixed buffer system consisting of glycerol, detergent, and phospholipid (Bogonez & Koshland, 1985). The loss in activity in detergent was not due to a decrease in the ligand binding affinity since detergent-solubilized receptor has been shown to bind to ligand with an affinity similar to that of membranous receptor samples (Biemann & Koshland, 1994; Lin et al., 1994). These results suggested that it was the cytoplasmic domain of the receptor which was sensitive to the buffer conditions and prompted us to test the effects of glycerol, phospholipid, and detergent on the stability of the c-fragment. Evidence of significant interaction between the c-fragment and these solutes is reported here. In the various surfactant-containing buffers that were tested, the conditions where cooperative transitions were observed correlated with the conditions where methylation of the intact receptor has been observed (Bogonez & Koshland, 1985), and in buffers where no receptor methylation was detected, no cooperative denaturation transition was observed. Thus the loss of receptor activity in detergent solution may be attributable to the deleterious effect of detergent on the tertiary (and quaternary) structure of the cytoplasmic domain of the receptor, and the restoration of activity in mixed buffers is probably due to the influence of glycerol on the CMC of OG and the positive stabilizing effect of glycerol on the protein.

MATERIALS AND METHODS

Chemicals, Bacterial Strains, and DNA Plasmids. *E. coli* lipids (acetone/ether precipitate) were obtained from Avanti Polar Lipids, Inc. (Alabaster, AL). Octyl β-D-glucopyranoside (OG) was obtained from Calbiochem (La Jolla, CA). All other chemicals used in these studies were reagent grade. JM103 (*supE thi-* Δ(*lac-proAB*), F′[*traD36 proAB lacI*^{q}]) and RP3808 (relevant genotype: Δ(*cheA-cheZ*)2209 *tsr-1*; Slocum & Parkinson, 1983) were used as host strains for the purification of the c-fragment using the pNC189 plasmid system described previously (Kaplan & Simon, 1988; Long & Weis, 1992). The mutant forms of the c-fragment used in this study are listed in Table 1. The aspartate receptor c-fragment was purified as previously described (Kaplan &

Simon, 1988; Long & Weis, 1992), and the concentration of the c-fragment was determined either by the BCA assay (Smith et al., 1985) or by using a value of ϵ_{280} determined previously (Long & Weis, 1992). JM103 and RP3808 (*cheRB*) were both used as host strains in preparations of the c-fragment. Since RP3808 lacked the methyltransferase (*cheR*) and the methylesterase (*cheB*) genes, it was used to make certain that neither the methyltransferase- nor the methylesterase-catalyzed covalent modification of the c-fragment occurred. No differences between the c-fragments isolated from either JM103 or RP3808 were ever detected by DSC; thus the c-fragments isolated from JM103 were judged not to be modified to any significant extent. To remove a persistent impurity in the preparations of the A436V tumble mutant c-fragment, an additional purification step was sometimes used and consisted of preparative GFC (TSK G3000SW, 21.5 mm i.d. × 60 cm) in phosphate buffer containing 5 M urea. The fractions containing the c-fragment were pooled, and the c-fragment was renatured by dialysis. The purity of the c-fragment samples was checked by sodium dodecyl sulfate–polyacrylamide gel electrophoresis, where highly-purified samples of the c-fragment resulted in the observation of a single band.

Analytical Size Exclusion Chromatography. The temperature dependence and reversibility of the oligomerization process for the S325L and S461L c-fragments were monitored by gel filtration chromatography since monomers and dimers could be separated by this method (Long & Weis, 1992). Proteins were eluted in 20 mM potassium phosphate/50 mM NaCl, pH 7.0 buffer at a flow rate of 0.7 mL/min using a Toso-Haas (Philadelphia, PA) TSK G3000SW$_{XL}$ column (8 mm i.d. × 30 cm) with void and included volumes of 5.5 and 12.5 mL, respectively. To determine the temperature dependence of the equilibrium constant for dimer dissociation of the S461L c-fragment, the c-fragment was incubated over a temperature range from 20 to 45 °C in 5 °C increments for 25 min at each temperature. At the end of each incubation interval an aliquot (typically 100 μL) was injected immediately to the gel filtration column at 4 °C, and the distribution of the protein among the monomer and dimer fractions was used to determine the equilibrium constant.

Differential Scanning Calorimetry. A Microcal MC2 differential scanning calorimeter (Microcal Inc., Northampton, MA) was used in all DSC experiments at a normalized scan rate of 72 °C/h. At the beginning of each scan, the sample and reference cells were brought to thermal equilibrium below 5 °C during a 65 min equilibration period using a refrigerated circulating bath to cool the calorimeter jacket. Specific heat capacity data were collected in scans from 5 to 95 °C. In a series of consecutive scans, the sample was cycled through the low-temperature equilibration period, scanned from 5 to 95 °C, and then cooled quickly back to the low starting temperature (since down scanning was not possible with our experimental setup).

Except for some experiments that were designed to explore the stability and reversibility of unfolding as a function of pH, pH 7.0 buffer was used which typically consisted of 20 mM potassium phosphate and 50 mM NaCl. Small variations in the concentration of phosphate (10 *versus* 20 mM) or the presence of divalent cation (10 mM $MgCl_2$) had no significant effects on stability. In some experiments, where noted, OG was added to the buffer. All protein solutions were dialyzed thoroughly against buffer, and dialysis buffer was used in the reference and sample cells to obtain a reference trace that was subtracted from the data during analysis.

DSC Data Analysis. Data were analyzed using the Origin software package (Microcal Software Inc., Northampton, MA) to carry out reference trace subtraction, concentration normalization, base-line construction and subtraction, and curve fitting. Prior to base-line subtraction the DSC traces could not be adequately fit by either a two-state or a non-two-state model which included provisions for an adjustable ΔC_p, and therefore a base-line subtraction procedure was adopted to obtain approximate values of the thermodynamics parameters. For the forms of the c-fragment that displayed only a single transition (wild-type, the E301K smooth mutant, and the tumble c-fragments V346M and V433I), this process consisted of two steps: subtracting a progress base line (Lin et al., 1993) from the normalized data followed by an analysis of the data with a non-two-state model to determine T_m and the van't Hoff and calorimetric enthalpies of denaturation, ΔH_{vH}^{den} and ΔH_{cal}^{den}, respectively (Sturtevant, 1987; see also the Appendix). ΔC_p was estimated from the normalized DSC traces before the progress base line was subtracted as the difference between the high- and low-temperature base lines extrapolated to the midpoint of the transition (T_m).

The denaturation (high-temperature) transitions of the oligomer-forming c-fragments (T311I, S325L, and S461L) were analyzed essentially as described above, but the analysis was modified to take into consideration the effect of the dissociation transition that occurred at lower temperatures. The fitted curves were obtained using the high-temperature region of the data since the excess heat capacity due to oligomer dissociation interfered with fits of the high-temperature transition. The value for the low-temperature cutoff was chosen to exclude the low-temperature transition and include as much of the data as possible below T_m of the high-temperature transition. An approximate value for the calorimetric enthalpy of dissociation, ΔH_{cal}^{dissoc}, was then estimated by extrapolating the fitted curve for the high-temperature transition to low temperatures and subtracting this from the entire data set. The remaining excess heat capacity at low temperature was integrated to obtain the value for the enthalpy of dissociation. This same method was also applied to the A436V tumble mutant c-fragment, which was also observed on occasion to possess a low-temperature transition.

Circular Dichroism Spectroscopy. For CD spectra and thermal denaturation curves, an Aviv 62DS circular dichroism spectrometer (Lakewood, NJ) was used. The sample was sandwiched between two Peltier units which regulated the temperature to a precision of ±0.2 °C. The temperature was recorded continuously by the voltage output of a T-type thermistor calibrated against the instrument's platinum resistance thermometer. For recording spectra, nitrogen was flushed through the lamp, monochromator, polarizer, and sample compartments at flow rates of 10, 20, 5, and 2 cfm, respectively. All CD experiments were performed in a cell of 0.1 mm (for wavelength scans) or 1 mm path length (for temperature scans). Wavelength scans were collected from 185 to 240 nm with a bandwidth of 1 nm and an averaging time of 10 s for each point. The averaging time was also 10 s for temperature scans at 222 nm, which were collected

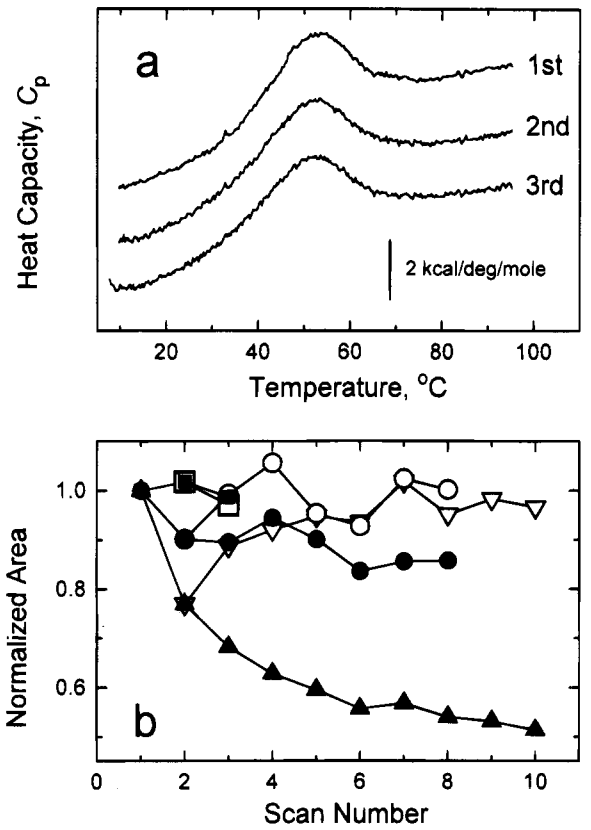

FIGURE 1: Reversibility of the c-fragment denaturation in pH 7 buffer (20 mM potassium phosphate, 50 mM NaCl, and 10 mM $MgCl_2$). (a) Three consecutive DSC traces (first, second, and third, top to bottom) of the wild-type c-fragment have had a buffer−buffer reference trace subtracted and were normalized to the initial protein concentration (5.7 mg/mL). The curves are offset for presentation. (b) Relative areas in the consecutive DSC traces for the wild-type (■, □), A436V (▲, ▽), and S461L (●, ○) c-fragments (5.7, 7.5, and 5.8 mg/mL, respectively). Closed symbols are relative areas normalized with respect to the first trace; open symbols are relative areas normalized with respect to the previous trace.

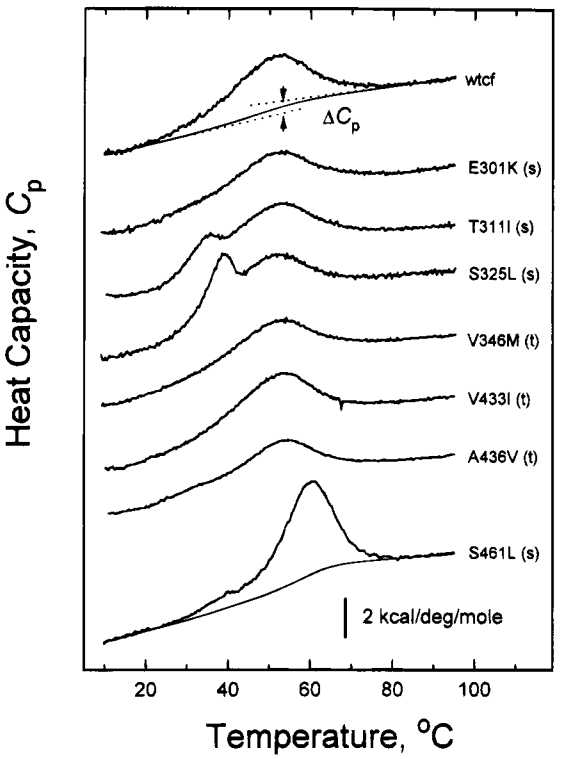

FIGURE 2: Normalized DSC traces of c-fragments for wild-type (wtcf), smooth (s), and tumble (t) mutants, as noted. Sample concentrations were 5.7, 4.5, 5.6, 4.1, 6.7, 6.3, 5.8, and 4.8 mg/mL (top to bottom). Examples of the progress base lines (—) that were used in base-line subtraction are drawn for the wild-type (wtcf) and S461L c-fragments. The DSC curves are offset for presentation. An example of the procedure for estimating ΔC_p, which is determined at T_m from the difference in extrapolated high- and low-temperature base lines, is illustrated in the DSC trace of the wtcf.

in either 1- or 3-deg intervals from 5 to 90 °C after an equilibration period of 3 min at the measurement temperature. A pH 7.0 buffer was used in all CD experiments, which consisted of 20 mM potassium phosphate and 50 mM NaCl. The buffer also contained, as noted, sonicated vesicles (2.0 mg/mL, prepared using a probe sonicator for 2 min at 150 W); OG (1−10 mg/mL); or glycerol (35% w/v). All spectra and temperature scans were processed by subtracting buffer scans taken under the same experimental conditions.

RESULTS

The c-Fragments Denature Reversibly. Normalized DSC traces are shown in Figure 1a for three consecutive scans of the wild-type c-fragment at a concentration of 5.7 mg/mL in pH 7.0 buffer. The calorimetric enthalpies obtained by integration were used as a measure of the reversibility of unfolding. Figure 1b plots the normalized areas determined from the DSC traces of the wild-type c-fragment (from Figure 1a) and two mutant c-fragments, A436V and S461L, all in pH 7.0 buffer. The closed symbols represent areas normalized with respect to the first DSC trace, and the open symbols are areas normalized with respect to the previous $(n - 1)$ trace. The latter normalization procedure quantifies the fraction of protein that has refolded after one DSC heating/cooling cycle. In phosphate buffer at pH 7.0, the reversibility of unfolding, relative to the preceding trace, was found to be ca. 95%. Reversibility of the wild-type c-fragment, tested as a function of the pH, was observed to decrease as the pH decreased. At pH 6.0 the reversibility was found to be ca. 80%, and at pH 5.5 denaturation was irreversible. It was also observed during the course of purification that the c-fragment precipitated below pH 5.5.

The unfolding transition for different c-fragments: wild-type, the smooth mutant c-fragments (E301K, T311I, S325L, and S461L), and the tumble mutant fragments (V346M, V433I, and A436V), are shown in Figure 2. Each of the c-fragments displayed in Figure 2 was determined to unfold reversibly in a minimum of two consecutive DSC scans. An approximate value for ΔC_p of 1 kcal/(mol·deg) was obtained from these data as illustrated in Figure 2 for the wild-type c-fragment (wtcf), by determining the difference between linear base lines at T_m, which were extrapolated from the high- and low-temperature regions of the DSC trace.

The DSC data in Figure 2 could not be adequately fit without first performing base-line subtraction. Three features of the data contributed to this situation: (i) the large transition width(s), (ii) the pronounced curvature in the low-temperature base-line region of the C_p trace, and (iii) the nonparallel nature of the low- and high-temperature base lines. After base line subtraction, these data were analyzed as a single transition using a non-two-state transition model. Examples of the progress baselines (Lin et al., 1993) which were subtracted from the normalized data are drawn in Figure 2 for the wild-type (wtcf) and the S461L smooth mutant

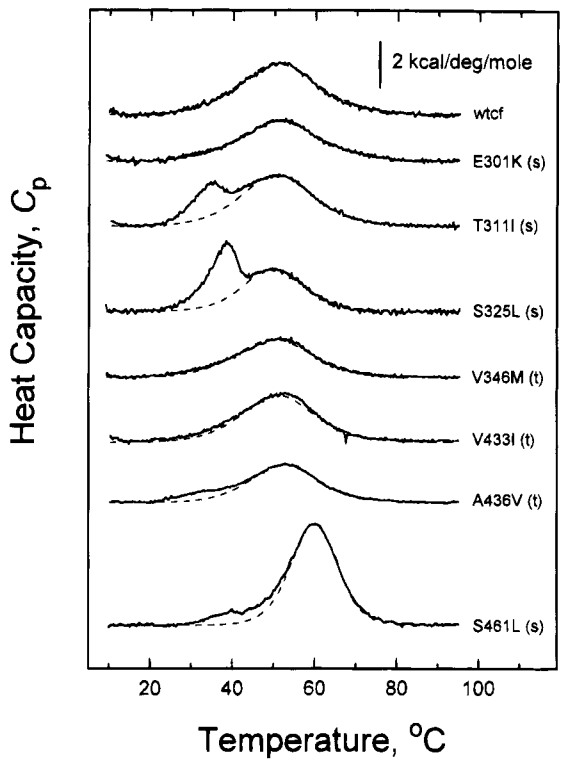

FIGURE 3: Base-line-subtracted, normalized DSC traces of c-fragments for wild-type (wtcf), smooth (s), and tumble (t) mutants, as noted. The main, high-temperature transitions were fit to a non-two-state model. For T311I, S325L, A436V, and S461L the low-temperature data were not included in the fits because of the excess C_p in these samples at the lower temperatures. The lower limits in the temperature ranges of the C_p data used in these fits were 45, 46, 43, and 54 °C, respectively. The DSC traces are offset for presentation.

c-fragment (the top and bottom traces, respectively). Base-line-subtracted DSC traces (solid lines) and the resulting fits (dashed lines) are plotted in Figure 3. The fits from these and other DSC traces (of the wild-type and A436V and S461L c-fragments) summarized in Table 1 indicated that the transition was approximately two-state, within the limits of our experimental error. Also, the observation of a well-defined isodichroic point in CD spectra of the wild-type c-fragment recorded as a function of temperature was consistent with a two-state transition (data not shown).

Two Transitions Are Observed for Oligomer-Forming c-Fragments. The tendency for certain single amino acid mutants of the c-fragment to form noncovalent dimers, and other oligomers, has been correlated with the receptor signaling state induced by the mutation (Long & Weis, 1992). While it was established that one particular mutation, a serine to leucine mutation at position 461 of the intact receptor (S461L), resulted in the formation of dimers, the numbers of subunits in the other clusters were not determined. We therefore refer to the clustered forms of the c-fragments as oligomers, except in the instances that are specific to the S461L c-fragment. Mutations which induced the smooth-swimming signaling state resulted in c-fragments with a strong tendency to form oligomers, and mutations that induced the tumble signaling state resulted in c-fragments that did not form clusters. This correlation has been extended to the number of transitions that were observed in the DSC and the formation of oligomers (see Figure 3). This low-temperature transition was quite evident in DSC traces of the T311I and S325L c-fragments, but was more subtle for the S461L c-fragment. Oligomers were not detected in GFC experiments for the "anomalous" E301K smooth mutant c-fragment (Long & Weis, 1992), an observation that was consistent with the absence of a second, low-temperature transition in the DSC traces of this c-fragment. Values of the calorimetrically-determined enthalpy of dissociation, ΔH_{cal}^{dissoc}, were obtained by the procedure described in Materials and Methods for the three smooth mutant c-fragments and are reported in Table 1.

Oligomer Formation Is Reversible. GFC was used to assess the reversibility of the association/dissociation reaction in samples of oligomer-forming c-fragments by determining the percent oligomer before and after incubating the sample at a temperature which favored monomer formation. For example, the S461L c-fragment was incubated at 50 °C for 25 min and then returned to 4 °C for 4 h (bottom trace in Figure 4a). The percent dimer in this sample (76%) was comparable to the percent dimer in a sample that was not heated (85%, Figure 4a, top trace). Measurements of the association and dissociation rate constants indicated that this heat-treated sample had probably not completely returned to equilibrium, since the rates were observed to have a large temperature coefficient, and at 4 °C the association/dissociation process has been found to be very slow (S. Seeley, G. Wittrock, L. Thompson, and R. Weis, unpublished results). As depicted in Figure 4b, a similar high level of reversibility was observed for the oligomer-forming smooth mutant S325L c-fragment. At 4 °C a 3 mg/mL solution of the S325L c-fragment was found to be 85% oligomer (calculated from the two major peaks in the top trace), and 81% oligomer for a 2 mg/mL solution (Figure 4b, second trace). When the temperature was shifted from 4 to 40 °C and the sample was incubated for 20 min, the c-fragment was predominantly monomeric (Figure 4b, third trace). A 3 mg/mL sample incubated at 40 °C for 20 min, and then returned to 4 °C for 4 h, was found to be 83% oligomer (Figure 4b, bottom trace). These experiments demonstrated that the association/dissociation process was highly reversible.

For the S461L c-fragment, the low-temperature transition was a subtle feature that was difficult to separate from the base line in the DSC traces, indicating a broad transition and a relatively small ΔH^{dissoc}. Even for the T311I and S325L c-fragments where the dissociation transitions were quite pronounced, the number of subunits participating in the dissociation process could not be determined from the heating curves since the peak shapes were probably affected by the kinetics of association/dissociation process, which is known to be slow in relation to the scan rate (S. Seeley, G. Wittrock, L. Thompson, and R. Weis, unpublished results). Independent estimates of the transition temperature and enthalpy for the dimer dissociation were obtained from the temperature dependence of the monomer−dimer equilibrium of the S461L c-fragment by gel filtration chromatography experiments. The GFC traces plotted in Figure 4a illustrate how the equilibrium between the S461L monomer and dimer varied as a function of temperature. T_m was estimated to be 35 °C from this experiment, since approximately equal masses of the monomer and dimer were in equilibrium at this temperature. The equilibrium dissociation constants determined from these data were used in a van't Hoff plot (Figure 4c) to estimate the enthalpy change of c-fragment

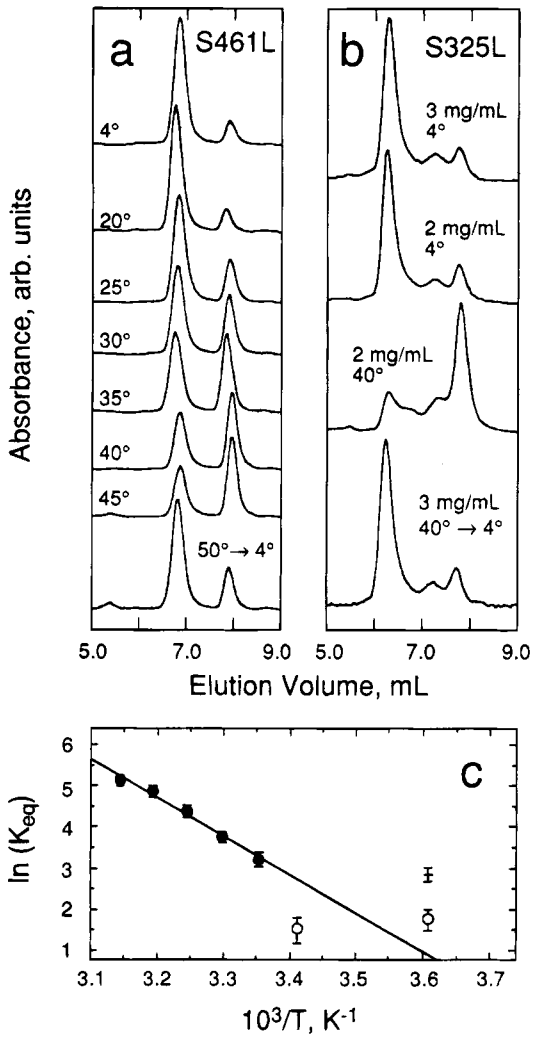

FIGURE 4: Gel filtration chromatography of oligomer-forming c-fragments. (a and b) Absorbance at 280 nm (arbitrary units) *versus* elution volume. The relative scales of the traces within each plot frame have been preserved, and the traces have been offset for clarity of presentation. GFC experiments were carried out in 20 mM potassium phosphate, 50 mM NaCl, and 10 mM $MgCl_2$, pH 7.0 buffer at a flow rate of 0.7 mL/min and 4 °C using samples that were preincubated under different temperature conditions. In panel a, 100 μL aliquots of the S461L c-fragment (3.75 mg/mL) were incubated for 25 min at the temperatures shown before being injected. In the bottom trace of panel a, the c-fragment was incubated for 25 min at 50 °C, followed by incubation at 4 °C for 150 min. In panel b the bottom two traces of the S325L c-fragment were obtained from samples incubated for 20 min at 40 °C. One sample (2 mg/mL) was injected directly; the other (3 mg/mL) was returned to 4 °C for an additional 4 h of incubation before injection. (c) van't Hoff analysis of the GFC data plotted in panel a. Data used in the fit (25 to 40 °C samples), ●; data not used in the fit, ○ (4 and 20 °C samples), + (50 → 4 °C sample). Error bars were determined assuming that the uncertainty in each peak (monomer or dimer) was 10% of the total peak area (monomer and dimer).

dissociation, ΔH_{vH}^{dissoc}, which was found to be 19 kcal/mol. The value of ΔH_{cal}^{dissoc} determined in DSC experiments was 12 kcal/mol (Table 1), which probably underestimated ΔH_{cal}^{dissoc} since the samples were not 100% dimer. That values for ΔH_{vH}^{dissoc} and ΔH_{cal}^{dissoc} are approximately equal is consistent with a previous study of c-fragments indicating that the clustered form of the S461L protein is a dimer (Long & Weis, 1992).

Oligomers Are More Completely Folded Than Monomers. Measurements of $[\theta]_{222}$ as a function of temperature are

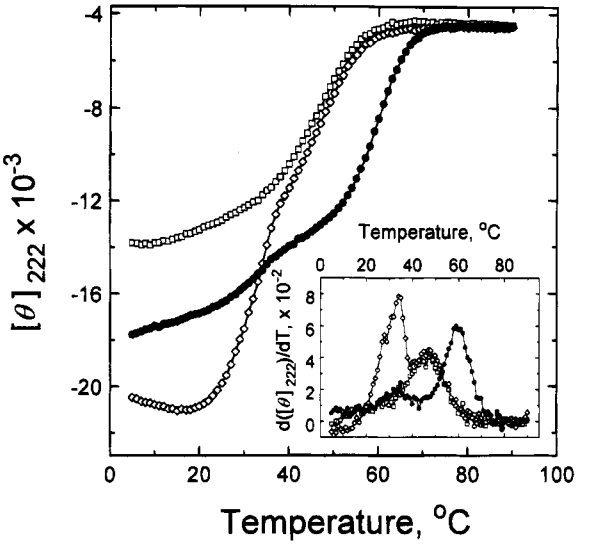

FIGURE 5: Mean residue ellipticity of the c-fragments as a function of temperature in 20 mM KP_i/50 mM NaCl, pH 7.0 buffer. $[\theta]_{222}$ is plotted as a function of temperature for the wild-type (□), S461L (●), and S325L (◇) c-fragments (all ca. 1.2 mg/mL). Inset: Temperature derivatives of the $[\theta]_{222}$ data.

plotted in Figure 5 for the wild-type, S325L, and S461L c-fragments. These data provided information about the relative amounts of apparent helical structure in the monomeric and oligomeric forms of the S461L and S325L c-fragments. With the S461L c-fragment a small but detectable loss in secondary structure occurs between 20 and 40 °C. By comparison, the apparent helix content of the S325L c-fragment decreased a large amount over the same range. The agreement between the temperature range over which the monomer−oligomer equilibria was observed to shift in GFC experiments, and the low-temperature transition range observed in DSC and θ_{222} *versus* temperature experiments, is evidence that the low-temperature transitions for the S325L and the S461L smooth mutant c-fragments are due to the dissociation of protein oligomers. The low-temperature transitions for both smooth mutant fragments were clearly discernible in the temperature derivative of $[\theta]_{222}$ plotted *versus* temperature (Figure 5 inset, with approximate low-temperature T_m's of 32 and 35 °C for the S325L and S461L c-fragments, respectively).

Comparison of the $[\theta]_{222}$ *versus* temperature data of the wild-type and S325L c-fragments (Figure 5) revealed that the S325L protein had significantly more secondary structure than the wild-type below 35 °C and that above the dissociation transition the two c-fragments behaved nearly identically. These observations provide evidence that the monomeric form of the S325L c-fragment is similar to the wild-type c-fragment and that additional structure is induced by oligomerization. In fact, all of the mutant c-fragments in their monomeric form (except S461L) are similar to the wild-type c-fragment on the basis of the DSC (Figures 2 and 3) and GFC experiments (Figure 4; Long & Weis, 1992). The oligomeric forms are, in contrast, more varied in their properties. As noted previously (Long & Weis, 1992), the clustered forms of the smooth mutant c-fragments exhibited significantly different elution profiles in GFC experiments (see also Figure 4). Also, the observed difference in $[\theta]_{222}$ of the two mutant forms in Figure 5 is consistent with different amounts of secondary structure in the oligomers,

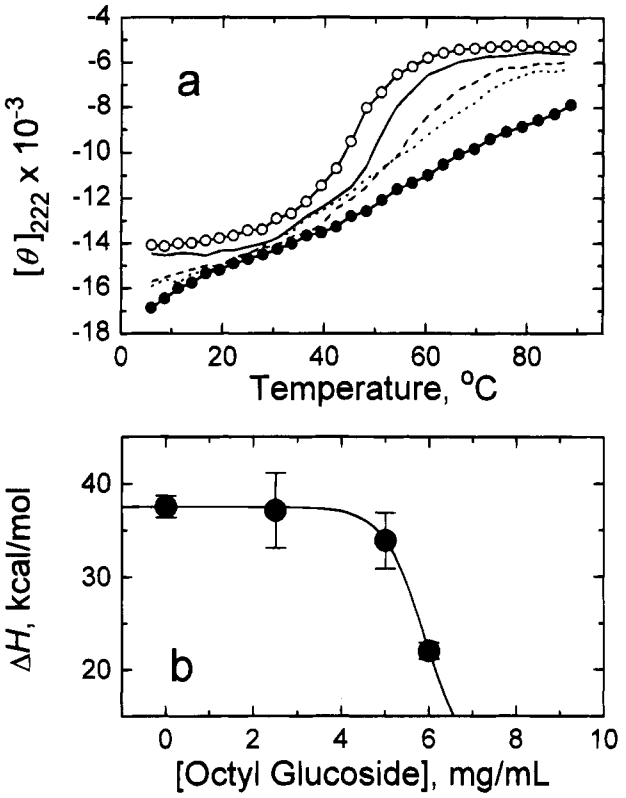

FIGURE 6: Mean residue ellipticity at 222 nm *versus* temperature for the wild-type c-fragment in OG-containing buffers. (a) θ_{222} is plotted as a function of temperature for a 0.4 mg/mL solution of the wild-type c-fragment in 20 mM KP_i/50 mM NaCl, pH 7.0 buffer (○), and with 2.5 (—), 5.0 (- - -), 7.0 (···), and 10 (●) mg/mL OG. (b) ΔH_{vH} as a function of OG concentration was determined from two independent sets of CD data using a two-state model. Error bars are standard errors of the mean.

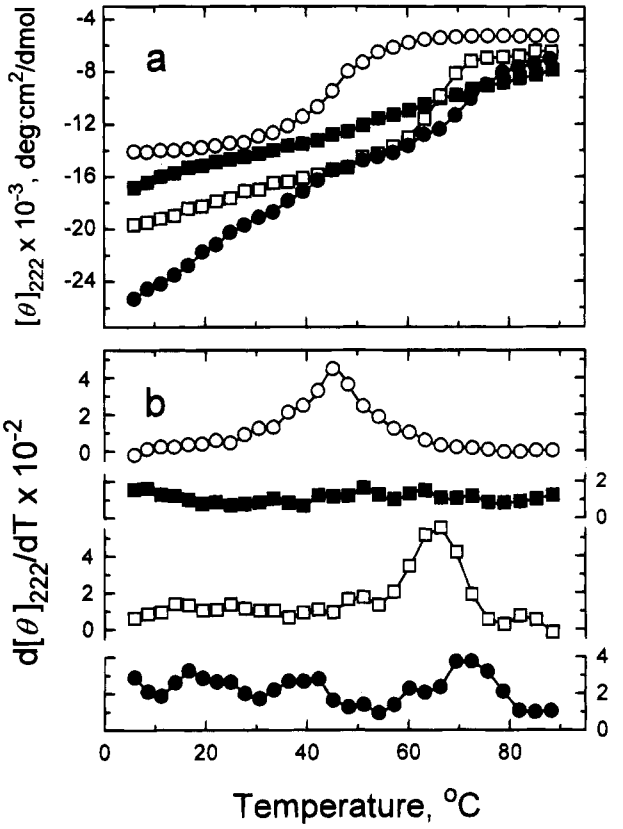

FIGURE 7: The effect of phospholipid and glycerol on the denaturation of c-fragment. Panel a: $[\theta]_{222}$ *versus* temperature for the wild-type c-fragment (ca. 0.3 mg/mL) in 20 mM KP_i/50 mM NaCl, pH 7.0 buffer (○); buffer plus 10 mg/mL OG (■); buffer plus 35% (w/v) glycerol (□); and buffer plus 2 mg/mL *E. coli* phospholipids, 35% glycerol, and 10 mg/mL OG (●). Panel b: Temperature derivatives of the CD data in panel a.

although a quantitative comparison using samples of known oligomer content is needed to verify this observation. Overall, a significant amount of unfolding appears to accompany oligomer dissociation, since the sign and magnitude of ΔH_{cal}^{dissoc} (Table 1) are most easily interpreted as a loss of structure, a view that is supported by the CD experiments.

Effects of Glycerol, Phospholipid, and Detergent on the c-Fragment. The influence of the buffer conditions on the wild-type c-fragment was studied by CD spectroscopy and DSC. Two effects of OG were observed in θ_{222} *versus* temperature experiments carried out as a function of the OG concentration (Figure 6). (1) At low OG concentrations (below 5 mg/mL) the transition temperature of c-fragment increased measurably (Figure 6a), ca. 5 °C with the addition of 5 mg/mL OG. (2) At higher concentrations of OG (greater than 6 mg/mL) the transition was broadened significantly, to the extent that the transition became undetectable at an OG concentration of 10 mg/mL. ΔH_{vH}^{den} determined using a two-state model (N = D) from an analysis of θ_{222} as a function of temperature was used to quantify this effect (Figure 6b). Analogous DSC experiments produced very similar results: (i) the width of the transition was unaffected below 5 mg/mL OG, but a measurable increase in T_m was observed, and (ii) for OG concentrations greater than 5 mg/mL, the transition broadened to the extent that it was indistinguishable from the base line at an OG concentration of 10 mg/mL (data not shown).

A simple explanation for these two observations can be made assuming that the protein behaves differently in detergent solutions below and above the CMC, which is ca. 6 mg/mL at 25 °C for OG (Jackson et al., 1982). At OG concentrations lower than the CMC, the c-fragment is stabilized by favorable binding interactions with OG monomers. Above the CMC the c-fragment interacts primarily with OG micelles, interactions that appear to reduce the cooperativity of protein denaturation. Interaction with OG micelles may cause a disruption of the protein tertiary structure, and not the secondary structure, an interpretation supported by the observation that the room temperature CD spectrum of the c-fragment is not significantly affected by the presence of 10 mg/mL OG in the buffer (data not shown). Also it is interesting to note that these effects are not shared by some coiled-coil proteins, as the thermal denaturation of tropomyosin is unaffected by the presence of 10 mg/mL OG (data not shown).

The effect of added glycerol on the c-fragment is qualitatively similar to the effect of OG at low concentrations: T_m was observed to increase 18 °C with the addition of 35% (w/v) glycerol (Figure 7). Tropomyosin was similarly stabilized by the addition of glycerol (data not shown). Phospholipids, on the other hand, had no detectable influence on the c-fragment. In thermal denaturation experiments monitored by θ_{222}, no change in the stability of the c-fragment (0.3 mg/mL) was observed by the addition of *E. coli* phospholipids (2 mg/mL, data not shown), indicating that there were no significant protein−lipid interactions.

However, the vesicle preparations were composed of an extract of *E. coli* lipids, and therefore the possibility that the c-fragment might have interacted with a particular class of lipid could not be excluded.

Mixtures of the wild-type c-fragment (0.3 mg/mL) with OG (10 mg/mL) and either glycerol (35% w/v) or both glycerol and phospholipid (2 mg/mL) produced effects on the c-fragment distinct from those observed with OG alone. The added effects of OG, phospholipid, and glycerol are shown in a θ_{222} *versus* temperature plot in Figure 7, which also shows for comparison the c-fragment in buffer with either glycerol, OG, or nothing added. As described above, a cooperative transition was undetectable in the OG/c-fragment mixture, but the apparent cooperativity could be partly restored by adding glycerol and phospholipid to an OG-containing sample. That similar data were obtained in buffer with OG and glycerol (but without added phospholipid) proved that the restoration of the transition was due primarily to the presence of glycerol, although the addition of phospholipid in combination with glycerol did have a modest effect in further restoring the transition. The restoration of the apparent cooperativity of the transition by glycerol in OG solutions may be explained by an increase in the CMC of OG in the presence of glycerol, since increases in the CMC of nonionic detergents have been observed to be a general effect of additives such as urea, ethylene glycol, and sugars (Kresheck, 1975; Meguro et al., 1987). Detergent, phospholipid, and glycerol combined with the c-fragment were also observed to markedly increase the magnitude of the CD signal at low temperatures at 222 nm. The underlying cause for the formation of this additional structure is not known.

DISCUSSION

Transmembrane signaling through receptor proteins couples a ligand-binding event on one side of the membrane to the cellular signaling apparatus on the other side. The crystal structure of the ligand-binding domain from the *S. typhimurium* aspartate receptor has provided a detailed picture of ligand binding (Milburn et al., 1991; Yeh et al., 1993). To understand the changes that occur in the cytoplasm, the properties of a 31-kDa cloned fragment derived from the cytoplasmic region of the *E. coli* aspartate receptor have been characterized. Through the use of mutants, it has been possible to study the effect of ligand binding indirectly, without the ligand-binding and transmembrane domains. The mutations are known to induce either a smooth-swimming or a tumbling bias in the chemotactic behavior of bacteria expressing the mutated receptor, by effectively "locking" the receptor into either the smooth-swimming (attractant-stimulated) or the tumble (repellent-stimulated) state (Mutoh et al., 1986; Ames & Parkinson, 1988). Our previous findings have correlated the mutations that induce the smooth-swimming behavioral bias, i.e., an attractant-stimulated receptor, with stronger subunit interactions in the c-fragment, which were shown to have a greater tendency to form clusters in solution (Long & Weis, 1992). In this study the reversibility of the association/dissociation and unfolding processes of the c-fragment, and the interactions of the c-fragment with phospholipids, glycerol, and OG, have been characterized with CD, DSC, and GFC. These data contribute to an understanding of the interactions between the receptor and the kinases CheA and CheW (Gegner et al., 1992; Schuster et al., 1993), which function together to regulate the phosphorylation levels of the response regulators CheY and CheB (Hess et al., 1998; Lupas & Stock, 1989; Borkovich & Simon, 1990).

Thermal Denaturation Properties of the c-Fragment. Conditions were found where dissociation and denaturation were over 90% reversible in all the c-fragments that were studied. The wild-type, one smooth mutant (E301K), and three tumble mutant c-fragments (A346M, V433I, A436V) display a single peak in DSC experiments. The T311I, S325L, and S461L smooth mutant c-fragments also have a low-temperature peak which is identified with oligomer dissociation. The main (high-temperature) peak of all of the c-fragments is characterized by similar values for T_m (51 °C), ΔH_{cal}^{den} (45 kcal/mol), and ΔC_p (1 kcal/(mol·deg)), with the exception of the S461L smooth mutant c-fragment which has a T_m at 60 °C. In all cases the high-temperature unfolding transition appears to be approximately two-state.

ΔH_{cal}^{den} and ΔC_p are unexpectedly small for a protein with a mass of the c-fragment (31 kDa). For small, reversibly-denaturing globular proteins, typical values of the specific enthalpy change, Δh_{cal}^{den}, and the specific heat capacity change, Δc_p, are ca. 6.5 cal/g and 0.12 cal/(g·deg), respectively (Haynie & Freire, 1993). The respective values for the c-fragment are ca. 1.5 cal/g and 0.03 cal/(g·deg). These small values might possibly be attributed to one or all of the properties that appear to be specific to this protein including (i) a nonglobular (fibrous) shape, (ii) incomplete folding due to fragmentation and/or the absence of the associated CheA and CheW proteins, and (iii) a highly dynamic structure (i.e., having some properties of a "molten globule" state).

That the predicted coiled-coil conformation (Lupas et al., 1991) could account for the small values of Δh_{cal}^{den} and Δc_p for the c-fragment is less likely in view of the values obtained for several coiled-coil proteins (Privalov, 1982), 6.3 cal/g and 0.07 cal/(g·deg), respectively. The small value of ΔH_{cal}^{den} observed for the c-fragment is more similar to ΔH_{cal}^{den} from molten globule states, which are often too small to be detected experimentally (reviewed in Haynie & Freire, 1993) and prohibits a direct comparison to the c-fragment. It may be the relatively large molecular mass of the c-fragment in relation to the other proteins used in calorimetry studies of the molten globule state (<20 kDa) that is partly responsible for our ability to detect ΔH_{cal}^{den}.

The anomolously small elution volume observed in GFC experiments is indicative of a value for the radius of gyration larger than would be expected for a tightly folded globular protein, but these data alone cannot distinguish between a protein in a nonglobular (e.g., fibrous) conformation, a protein that is unusually dynamic and/or partly unfolded, or both. Evidence for the dynamic and/or partly unfolded nature of the monomeric form of the c-fragment has been obtained in preliminary NMR experiments which have shown that nearly all of the amide protons are in rapid exchange with water (Seeley et al., 1994).

Properties of the c-Fragment Oligomers. Mutations in a number of the chemotaxis genes (e.g., *cheA, cheW, cheY, cheZ, cheR, cheB, tar, tsr*) produce the smooth and tumble bias phenotypes (Macnab, 1987). The mutations in the receptor genes can undoubtedly produce the smooth and tumble biases through different aspects of receptor function,

for example, by inducing changes in either protein conformation or protein−protein interactions. The similar stability of the wild-type, smooth, and tumble c-fragments (except S461L) can be interpreted as negative evidence for changes in protein conformation that can be detected by changes in protein stability. Alternatively, the changes in the signaling state may be produced by changes in protein−protein interactions, either between subunits of the receptor, or between the receptor and the other chemotaxis protein, e.g., CheA and CheW, changes which may be less likely to affect the stability of isolated subunits. The only correlation between c-fragment structure and receptor signaling state known presently is the tendency for the smooth mutant c-fragments to form oligomers (Long & Weis, 1992).

Based on the data from the DSC, CD, and gel filtration experiments of the set of mutants analyzed in this study, three generalizations regarding c-fragment structure may be stated: (i) the clustered forms are more fully folded than the monomeric forms, (ii) the structure of the clustered form is dependent on the mutation that induces cluster formation, and (iii) the structure of the monomeric form is largely unaffected by the mutations which influence clustering.

Lipid−c-Fragment Interactions. The cytoplasmic domain is normally anchored near the surface of the bilayer membrane in the intact receptor and is either complexed to or in communication with the kinase (CheA), CheW, the methylesterase (CheB), and the methyltransferase (CheR). A marked effect of lipids on the properties of the c-fragment is expected if there are significant interactions between the membrane and cytoplasmic domain of the receptor. Our measurements of the influences of added surfactants and glycerol on the thermal stability indicate that the nonionic detergent OG and glycerol have marked effects on the properties of the c-fragment, but that *E. coli* lipids have little influence. The varied nature of the effects produced by OG are unexpected, but a plausible explanation is based on different modes of interaction between the c-fragment and OG below and above the CMC.

The influence of OG on receptor methylation activity may be explained using the results reported here. Bogonez and Koshland (1985) found that membranous samples of the *S. typhimurium* aspartate receptor were efficiently methylated in a reaction with *S*-adenosyl-L-methionine catalyzed by the methyltransferase, but methylation could not detected in receptor samples solubilized with OG above the CMC. Methylation activity could be restored in a "solubilized", mixed buffer system consisting of OG, phospholipid, and glycerol. In this study we have observed that the c-fragment exhibits a cooperative transition under the same conditions where receptor methylation can be observed, suggesting that the receptor retains sufficient structure in the presence of phospholipids, glycerol, and detergent to be a substrate for methylation. The ability of the receptor to be a substrate in the methylation reaction in the mixed glycerol−detergent−lipid system appears to be a direct consequence of the stabilizing influence of glycerol which can counteract the effects of OG. The sensitive nature of this receptor system to a mild nonionic detergent suggests that hyrdophobic interactions in the receptor are critically important for the transmembrane signaling activity and that alternative strategies for producing a solubilized receptor system need to be developed.

APPENDIX

Determination of ΔH_{cal}^{den} and ΔH_{vH}^{den} from DSC Data. The excess heat capacity, C_p^{ex}, of a protein unfolding as a function of temperature is given by

$$C_p^{ex}(T) = \Delta H_{cal}^{den}\left(\frac{\delta f_{den}}{\delta T}\right) \tag{A1}$$

where ΔH_{cal}^{den} is the calorimetric enthalpy of unfolding and f_{den} is the unfolded fraction of protein. Equation A1 applies to the specific case of a single transition, where the change in heat capacity of unfolding is assumed to be zero (which is the case for the base-line-corrected DSC traces). The van't Hoff enthalpy (ΔH_{vH}^{den}) and ΔH_{cal}^{den} are not held equal in fitting heat capacity data from DSC experiments to a non-two-state model. ΔH_{cal}^{den} is determined from direct numerical integration of C_p^{ex}, in the normalized, baseline-corrected data. ΔH_{vH}^{den} is estimated from relationships between the equilibrium constant (K_{den}) for the overall unfolding process (N = D) and the experimental C_p data as a function of temperature. The fractions of unfolded (f_{den}) and native (f_{nat}) protein in the sample are proportional the areas under the C_p curve, below and above, respectively, the temperature where K_{den} is evaluated. f_{den} can be expressed in terms of K_{den} ($f_{den} = K_{den}/(1 + K_{den})$), and thus the temperature derivative of f_{den} can be written as

$$\frac{\delta f_{den}}{\delta T} = \frac{K_{den}}{(1 + K_{den})^2}\frac{\delta(\ln K_{den})}{\delta T} \tag{A2}$$

Making use of the van't Hoff relation and inserting the expression for $\delta f_{den}/\delta T$ into the equation for C_p^{ex} (eq A1), a relation between ΔH_{vH}^{den} and the C_p data is obtained.

$$C_p^{ex}(T) = \Delta H_{cal}^{den}\frac{K_{den}}{(1 + K_{den})^2}\frac{\Delta H_{vH}^{den}}{RT^2} \tag{A3}$$

K_{den} is determined from the van't Hoff equation:

$$K_{den}(T) = \exp\left\{\frac{-\Delta H_{vH}^{den}}{RT}\left(1 - \frac{T}{T_m}\right)\right\} \tag{A4}$$

integrated between the transition midpoint, T_m (where the reaction is half complete and $K_{den} = 1$), to some specified temperature, T. Equations A3 and A4 form the basis for the fitting routine. Initial estimates of ΔH_{vH}^{den} and T_m are used to calculate $C_p^{ex}(T)$, which are used with the experimental values of $C_p^{ex}(T)$ to determine χ^2. Using Marquardt nonlinear least-squares methods, ΔH_{vH}^{den} and T_m are varied iteratively until no further reduction in χ^2 is obtained.

ACKNOWLEDGMENT

The authors thank Dr. John F. Brandts for helpful discussions and comments on the manuscript.

REFERENCES

Ames, P., & Parkinson, J. S. (1988) *Cell 55*, 817−826.
Biemann, H.-P., & Koshland, D. E., Jr. (1994) *Biochemistry 33*, 629−634.
Bogonez, E., & Koshland, D. E., Jr. (1985) *Proc. Natl. Acad. Sci. U.S.A. 82*, 4891−4895.

Borkovich, K. A., & Simon, M. I. (1990) *Cell 63*, 1339−1348.
Bourret, R. B., Borkovich, K. A., & Simon, M. I. (1991) *Annu. Rev. Biochem. 60*, 401−441.
Dahl, M. K., & Manson, M. D. (1985) *J. Bacteriol. 164*, 1057−1063.
Gegner, J. A., Graham, D. R., Roth, A. F., & Dahlquist, F. W. (1992) *Cell 70*, 975−982.
Haynie, D. T., & Freire, E. (1993) *Protein Struct., Funct., Genet. 16*, 115−140.
Hazelbauer, G. L. (1992) *Curr. Opin. Struct. Biol. 2*, 505−510.
Hazelbauer, G. L., Yaghami, R., Burrows, G. G., Baumgartner J. W., Dutton, D. P., & Morgan, D. G. (1990) in *Biology of the Chemotactic Response* (Armitage, J. P., & Lackie, J. M., Eds.) Society for General Microbiology Symposium Vol. XLVI, pp 107−134, Cambridge University Press, Cambridge, England.
Hess, J. F., Oosawa, K., Kaplan, N., & Simon, M. I. (1988) *Cell 53*, 79−87.
Jackson, M. L., Schmidt, C. F., Lichtenberg, D., Litman, B. J., & Albert, A. D. (1982) *Biochemistry 21*, 4576−4582.
Kaplan, N., & Simon, M. I. (1988) *J. Bacteriol. 170*, 5134−5140.
Kehry, M. R., Engstrom, P., Dahlquist, F. W., & Hazelbauer, G. L. (1983) *J. Biol. Chem. 258*, 5050−5055.
Kresheck, G. C. (1975) in *Water, A Comprehensive Treatment, Volume 4, Aqueous Solutions of Amphiphiles and Macromolecules* (Franks, F., Ed.) pp 95−167, Plenum Press, New York.
Lin, L.-N., Mason, A. B., Woodworth, R. C., & Brandts, J. F. (1993) *Biochem. J. 293*, 517−522.
Lin, L.-N., Li, J., Brandts, J. F., & Weis, R. M. (1994) *Biochemistry 33*, 6564−6570.
Liu, J., & Parkinson, J. S. (1991) *J. Bacteriol. 173*, 4941−4951.
Long, D. G., & Weis, R. M. (1992) *Biochemistry 31*, 9904−9911.
Lupas, A., & Stock, J. (1989) *J. Biol. Chem. 264*, 17337−17342.
Lupas, A., Van Dyke, M., & Stock, J. (1991) *Science 252*, 1162−1164.
Macnab, R. M. (1987) in *Escherichia coli and Salmonella typhimurium. Cellular and Molecular Biology* (Neidhardt, F. C., Ed.) Vol. 1, pp 732−759, American Society for Microbiology Press, Washington, DC.
Meguro, K., Ueno, M., & Esumi, K. (1987) in *Nonionic Surfactants. Physical Chemistry. Surfactant Science Series Volume 23* (Schick, M. J., Ed.) pp 109−183, Marcel Dekker, New York.
Milburn, M. V., Privé, G. G., Milligan, D. L., Scott, W. G., Yeh, J., Jancarik, J., Koshland, D. E., Jr., & Kim, S.-H. (1991) *Science 254*, 1342−1347.
Milligan, D. L., & Koshland, D. E., Jr. (1988) *J. Biol. Chem. 263*, 6268−6275.
Mutoh, N., Oosawa, K., & Simon, M. I. (1986) *J. Bacteriol. 167*, 992−998.
Nowlin, D. M., Bollinger, J., & Hazelbauer, G. L. (1987) *J. Biol. Chem. 262*, 6039−6045.
Nowlin, D. M., Bollinger, J., & Hazelbauer, G. L. (1988) *Proteins 3*, 102−112.
Oosawa, K., Mutoh, N., & Simon, M. I. (1988) *J. Bacteriol. 170*, 2521−2526.
Pakula, A. A., & Simon, M. I. (1992) *Proc. Natl. Acad. Sci. U.S.A. 89*, 4144−4148.
Parkinson, J. S. (1993) *Cell 73*, 857−871.
Privalov, P. L. (1982) *Adv. Protein Chem. 35*, 1−104.
Schuster, S. C., Swanson, R. V., Alex, L. A., Bourret, R. B., & Simon, M. I. (1993) *Nature 365*, 343−347.
Seeley, S. K., Weis, R. M., & Thompson, L. K. (1994) *Biophys. J. 66*, A172.
Slocum, M. K., & Parkinson, J. S. (1983) *J. Bacteriol. 155*, 565−577.
Smith, P. K., Krohn, R. I., Hermanson, G. T., Mallia, A. K., Gartner, F. H., Provenzano, M. D., Fujimoto, E. K., Goeke, N. M., Olson, B. J., & Klenk, D. C. (1985) *Anal. Biochem. 150*, 76−85.
Stewart, R. C., & Dahlquist, F. W. (1987) *Chem. Rev. 87*, 997−1025.
Stock, J. B., Lukat, G. S., & Stock, A. M. (1991) *Annu. Rev. Biophys. Biophys. Chem. 20*, 109−136.
Sturtevant, J. M. (1987) *Annu. Rev. Phys. Chem. 38*, 463−488.
Terwilliger, T. C., Bogonez, E., Wang, E. A., & Koshland, D. E., Jr. (1983) *J. Biol. Chem. 258*, 9608−9611.
Terwilliger, T. C., Wang, J. Y., & Koshland, D. E., Jr. (1986) *Proc. Natl. Acad. Sci. U.S.A. 83*, 6707−6710.
Tso, W. W., & Adler, J. (1974) *J. Bacteriol. 118*, 560−576.
Yeh, J. I., Biemann, H.-P., Pandit, J., Koshland, D. E., Jr., & Kim, S.-H. (1993) *J. Biol. Chem. 268*, 9787−9792.

BI9423648